ISSN 1749-3889 (print), 1749-3897 (online)
International Journal of Nonlinear Science
Vol.4(2007) No.3,pp.171-185

Bifurcation Analysis, Chaos and Control in the Burgers Mapping

E. M. ELabbasy, H. N. Agiza, H. EL-Metwally, A. A. Elsadany *
Department of Mathematics, Faculty of Science, Mansoura University
Mansoura 35516, Egypt
(Received 18 April 2007, accepted 29 June 2007)

Abstract: In this paper, the bifurcation analysis for Burgers mapping has been studied. The existence and stability of the fixed points of this map was derived. The conditions of existence for pitchfork bifurcation, flip bifurcation and Neimark-Sacker bifurcation are derived by using center manifold theorem and bifurcation theory. The control of the map around stable Neimark-Sacker bifurcation has been achieved by using feedback polynomial controller technique. The complex dynamics, bifurcations and chaos are displayed by numerical simulations.

Key words: Burgers mapping; Neimark-Sacker bifurcation; Chaotic behavior; feedback controller of polynomial functions

1 Introduction

The Burgers mapping is a discretisation of a pair of coupled differential equations which were used by Burgers [1] to illustrate the relevance of the concept of bifurcation to the study of hydrodynamics flows. These equations are indeed a sort of Lorenz model; being in two dimensions they cannot exhibit complex trajectories (see [2]). The Burgers mapping is defined in the following way [2,3]:

$$\begin{cases} x_{n+1} = (1-\nu)x_n - y_n^2, \\ y_{n+1} = (1+\mu)y_n + x_n y_n. \end{cases} \tag{1}$$

In [3], the map (1) has been discussed by using the numerical methods. They proved numerically, that Burgers mapping are produced a much richer set of dynamic patterns than those observed in continuous case [3,2]. Nevertheless, they have not given theoretical analysis. In this paper we deduce theoretical analysis for bifurcations phenomenon and the polynomial type controller [4] to achieve control of chaotic attractor around stable Neimark-Sacker bifurcation for map (1). Jing group have been applied the forward Euler scheme for the BVP oscillator, FitzHugh-Nagumo system and Predator-prey [5,6,7], they investigated the dynamical behaviors in detail as discrete dynamical systems by using the qualitative analysis and center manifold theorem. In addition, Bifurcations and chaos of the delayed ecological model has been examined in [8]. Recently, Zhang et al. applied the forward Euler scheme for the simple predator-prey model [9], and they studied the dynamical behaviors by using the qualitative analysis and center manifold theorem.

This paper is organized as follows. In section 2, the existence and stability of the fixed points and the qualitative behavior and bifurcations of the map (1) are examined by using the qualitative theory and bifurcation theory. Also, the conditions of existence for pitchfork bifurcation, flip bifurcation and Neimark-Sacker bifurcation deduced and proved. In section 3, we applied the controller technique of Chen-Yu [4] for control this map around stable Neimark-Sacker bifurcation. In section 4, the complex behaviors for the map via computing bifurcation diagrams, strange attractors and Lyapunov exponents by numerical simulations were demonstrated. Finally, section 5 draws the conclusion.

*Corresponding author. *E-mail address*: aelsadany1@yahoo.com

IJNS.2007.12.15/109

2 Existence and stability of fixed points and bifurcations

In this section, we first determine the existence of the fixed points of the map (1), then investigate their stability by calculating the eigenvalues for the Jacobian matrix of the map (1) at each fixed point, and sufficient conditions of existence for pitchfork bifurcation flip bifurcation and Neimark-Sacker bifurcation by using qualitative theory and bifurcation theory.

By simple computation, the map (1) has the following three fixed points:

(i) $E_0(0,0)$ is trivial fixed point,

(ii) $E_1(-\mu, \sqrt{\mu\nu})$ is interior fixed point exist for $\mu\nu > 0$, and

(iii) $E_2(-\mu, -\sqrt{\mu\nu})$ is the other interior fixed point. Where E_1 and E_2 are symmetric fixed points of coordinates.

Next we will investigate qualitative behaviors of the map (1). The local dynamics of map (1) in a neighborhood of a fixed point is dependent on the Jacobian matrix of (1). The Jacobian matrix of map (1) at the state variable is given by

$$J(x,y) = \begin{pmatrix} 1-\nu & -2y \\ y & 1+\mu+x \end{pmatrix}. \tag{2}$$

2.1 Bifurcations of $E_0(0,0)$

We consider the Jacobian matrix at E_0 which has the form

$$J(E_0) = \begin{pmatrix} 1-\nu & 0 \\ 0 & 1+\mu \end{pmatrix}, \tag{3}$$

which has two eigenvalues $\lambda_1 = 1-\nu$ and $\lambda_2 = 1+\mu$. From the above one can make conclusions:

Proposition 1 *(1) When $0 < \nu < 2$ and $-2 < \mu < 0$, E_0 is a stable node (sink); (2) When $\nu > 2$ and $\mu > 0$, E_0 is unstable node (source); (3) When $\nu > 2$ and $-2 < \mu < 0$,or when $0 < \nu < 2$ and $\mu > 0$, E_0 is saddle point; (4) When $\nu = 0$ or 2 and $|\lambda_2| \neq 1$ or $\mu = -2$ or $\mu = 0$ and $|\lambda_1| \neq 1$, E_0 is a non-hyperbolic fixed point.*

Considering that μ is a bifurcation parameter, and E_0 is a non-hyperbolic fixed point for $\mu = 0$ or $\mu = -2$, so the stability and bifurcations will be discussed in the following part.

If $\mu = 0$, then $J(E_0)$ has two eigenvalues $\lambda_1 = 1-\nu$ and $\lambda_2 = 1$. The fact that the fixed point E_0 is a pitchfork bifurcation point requires the following proposition.

Proposition 2 *If $\mu = 0$ and $\nu \neq 0$, the map (1) undergoes a pitchfork bifurcation at E_0. Moreover the map has only one fixed point.*

Proof. Let $\sigma_n = \mu$, such that parameter σ_n be a new dependent variable, the map (1) can be rewritten in the following form:

$$\begin{pmatrix} x_{n+1} \\ \sigma_{n+1} \\ y_{n+1} \end{pmatrix} = \begin{pmatrix} 1-\nu & 0 & 0 \\ 0 & 1 & 0 \\ 0 & 0 & 1 \end{pmatrix} \begin{pmatrix} x_n \\ \sigma_n \\ y_n \end{pmatrix} + \begin{pmatrix} -y_n^2 \\ 0 \\ x_n y_n + \sigma_n y_n \end{pmatrix}.$$

By the center manifold theory there exists a center manifold of the map (1), which can expressed locally as follows:

$$W^c(E_0) = \{(x,y,\sigma) \in R^3 \,|\, y = w(x,\sigma), w(0,0) = Dw(0,0) = 0, |x| < \varepsilon, |y| < \delta\},$$

Assume that $w(y,\sigma)$ has the following form

$$x_n = w(y_n, \sigma_n) = a_1 y_n^2 + a_2 y_n \sigma_n + a_3 \sigma_n^2 + o((|x_n| + |y_n|)^3),$$

which must satisfy

$$w(y + y_n w + y_n \sigma_n, \sigma_{n+1}) = (1-\nu)w - y_n^2.$$

Thus, we can obtain that

$$a_1 = -\frac{1}{\nu} \quad \text{and} \quad a_2 = a_3 = 0,$$

therefore, we have $x_n = w(y_n, \sigma_n) = -\frac{1}{\nu}x_n^2$, and the map is restricted to the center manifold, which given by

$$f_1 : y_{n+1} = y_n + \sigma_n y_n - \frac{1}{\nu}y_n^3 - o((|y_n| + |\sigma_n|)^4).$$

Since $\frac{\partial^2 f_1}{\partial y_n \partial \sigma_n}\big|_{(0,0)} = 1 \neq 0$, $\frac{\partial^3 f_1}{\partial y_n^3}\big|_{(0,0)} = -\frac{6}{\nu} \neq 0$ and $\tilde{f}_1(y, \sigma) = y + \sigma y - \frac{1}{\nu}y^3$ is odd function for y, then map (1) undergoes a pitchfork bifurcation at E_0. If $\nu > 0$, then the map (1) undergoes a supercritical pitchfork bifurcation, whereas the map (1) undergoes a subcritical pitchfork bifurcation when $\nu < 0$.This completes the proof ■

Now the flip bifurcation of the map (1) at E_0 is considered. If $\mu = -2$, then $J(E_0)$ has two eigenvalues $\lambda_1 = 1 - \nu$ and $\lambda_2 = -1$. The fact that the fixed point E_0 is a flip bifurcation point is given by the following proposition.

Proposition 3 *If $\mu = -2$, $\nu \neq 0$, the map (1) undergoes a flip bifurcation at E_0.*

Let $\sigma_n = \mu + 2$, such that parameter σ_n be a new dependent variable, the map (1) can be rewritten in the following form:

$$\begin{pmatrix} x_{n+1} \\ \sigma_{n+1} \\ y_{n+1} \end{pmatrix} = \begin{pmatrix} 1-\nu & 0 & 0 \\ 0 & -1 & 0 \\ 0 & 0 & -1 \end{pmatrix} \begin{pmatrix} x_n \\ \sigma_n \\ y_n \end{pmatrix} + \begin{pmatrix} -y_n^2 \\ 0 \\ x_n y_n + \sigma_n y_n \end{pmatrix}.$$

Assume that $w(y, \sigma)$ has the following form:

$$x_n = w(y_n, \sigma_n) = b_1 y_n^2 + b_2 y_n \sigma_n + b_3 \sigma_n^2 + o((|y_n| + |\sigma_n|)^3).$$

It must satisfy

$$w(-y_n + y_n w + \sigma_n y_n, \sigma_{n+1}) = (1 - \nu)w - y_n^2.$$

Thus, we can obtain that

$$b_1 = -\frac{1}{\nu} \text{ and } b_2 = b_3 = 0,$$

therefore, we have $x_n = w(y_n, \sigma_n) = -\frac{1}{\nu}y_n^2$, and the map is restricted to the center manifold, which given by

$$f_2 : y_{n+1} = -y_n + \sigma_n y_n - \frac{1}{\nu}y_n^3 - o((|\sigma_n| + |y_n|)^4).$$

Since

$$\begin{aligned} \alpha_1 &= (\frac{\partial f_2}{\partial \sigma_n}\frac{\partial^2 f_2}{\partial y_n^2} + 2\frac{\partial^2 f_2}{\partial y_n \partial \sigma_n})\big|_{(0,0)} = 2 \neq 0, \\ \alpha_2 &= (\frac{1}{2}(\frac{\partial^2 f_2}{\partial y_n^2})^2 + \frac{1}{3}\frac{\partial^3 f_2}{\partial y_n^3})\big|_{(0,0)} = -\frac{2}{\nu} < 0, \end{aligned}$$

then map (6.1) undergoes a flip bifurcation at E_0. If $\nu > 0$, then the map (1) undergoes a supercritical flip bifurcation, whereas the map (1) undergoes a subcritical bifurcation when $\nu < 0$. This complete the proof ■

2.2 Bifurcation of fixed point $E_1(-\mu, \sqrt{\mu\nu})$

We consider the Jacobian matrix at E_1 which has the form

$$J(E_1) = \begin{pmatrix} 1-\nu & -2\sqrt{\nu\mu} \\ \sqrt{\nu\mu} & 1 \end{pmatrix}, \tag{4}$$

which has two eigenvalues $\lambda_{1,2} = \frac{1}{2}(2-\nu \pm \sqrt{(2-\nu)^2 - 4(1-\nu+\nu\mu)})$. $E_1(-\mu, \sqrt{\mu\nu})$ is nontrivial fixed point. Under certain conditions, it can be obtained that map (1) also undergoes pitchfork bifurcation and flip bifurcation at $E_1(-\mu, \sqrt{\mu\nu})$. This will be shown by the following two propositions.

Proposition 4 *If $\nu^2 - 4\mu\nu > 0$ and $\mu = 0$, the map (1) undergoes a pitchfork bifurcation at E_1. Moreover the map has only one fixed point.*

Proof. The proof is similar to the proof of proposition 2. ■

Proposition 5 *If $\nu^2 - 4\mu\nu > 0$ and $\mu = \dfrac{\nu-2}{\nu}$, $\nu \neq 2$ the map (1) undergoes a flip bifurcation at E_1.*

Proof. In order to prove this result, we consider the eigenvalues of Jacobian matrix at E_1 which has the form

$$J(E_1) = \begin{pmatrix} 1-\nu & -2\sqrt{\nu\mu} \\ \sqrt{\nu\mu} & 1 \end{pmatrix},$$

which has two eigenvalues are $\lambda_{1,2} = \frac{1}{2}(2-\nu \pm \sqrt{(2-\nu)^2 - 4(1-\nu+\nu\mu)})$. For $\mu = \frac{\nu-2}{\nu}$, the two eigenvalues becomes $\lambda_1 = 3-\nu$ and $\lambda_2 = -1$.

Let $\zeta_n = x_n + \nu$, $\eta_n = y_n - \sqrt{\nu\mu}, \sigma_n = \sqrt{\mu} - \sqrt{\frac{\nu-2}{\nu}}$ and σ_n be a new dependent parameters, the map (1) becomes

$$\begin{pmatrix} \zeta_{n+1} \\ \sigma_{n+1} \\ \eta_{n+1} \end{pmatrix} = \begin{pmatrix} 1-a & 0 & -2\sqrt{\nu-2} \\ 0 & -1 & 0 \\ \sqrt{\nu-2} & 0 & 1 \end{pmatrix} + \begin{pmatrix} 2\sqrt{\nu}\sigma_n\eta_n - \eta_n^2 \\ 0 \\ \sqrt{\nu}\sigma_n\zeta_n + \zeta_n\eta_n \end{pmatrix}. \tag{5}$$

Let

$$T = \begin{pmatrix} -\sqrt{\nu-2} & 0 & 1 \\ 0 & 1 & 0 \\ 1 & 0 & -\dfrac{\sqrt{\nu-2}}{2} \end{pmatrix}.$$

By the following transformation

$$\begin{pmatrix} \zeta_n \\ \sigma_n \\ \eta_n \end{pmatrix} = T \begin{pmatrix} u_n \\ \delta_n \\ \vartheta_n \end{pmatrix}$$

the map (5) becomes

$$\begin{pmatrix} u_{n+1} \\ \delta_{n+1} \\ \vartheta_{n+1} \end{pmatrix} = \begin{pmatrix} (3-\nu) & 0 & 0 \\ 0 & -1 & 0 \\ 0 & 0 & -1 \end{pmatrix} \begin{pmatrix} u_n \\ \delta_n \\ \vartheta_n \end{pmatrix} + \begin{pmatrix} \psi(u_n, \delta_n, \vartheta_n) \\ 0 \\ \phi(u_n, \delta_n, \vartheta_n) \end{pmatrix}, \tag{6}$$

where

$$\psi(u_n, \delta_n, \vartheta_n) = \frac{4\sqrt{\nu}\sqrt{\nu-2}}{\nu-4}\delta_n u_n - \frac{\nu\sqrt{\nu}}{\nu-4}\delta_n\vartheta_n + \frac{3\sqrt{\nu-2}}{\nu-4}u_n^2 - \frac{2(\nu-1)}{\nu-4}u_n\vartheta_n + \frac{(\nu-2)\sqrt{\nu-2}}{\nu-4}\vartheta_n^2$$

$$\phi(u_n, \delta_n, \vartheta_n) = \frac{2\nu\sqrt{\nu}}{\nu-4}\delta_n u_n - \frac{4\sqrt{\nu}\sqrt{\nu-2}}{\nu-4}\delta_n\vartheta_n + \frac{2(\nu-1)}{\nu-4}u_n^2 - \frac{(\nu+2)\sqrt{\nu-2}}{\nu-4}u_n\vartheta_n + \frac{3(\nu-2)}{2(\nu-4)}\vartheta_n^2$$

Consider

$$u_n = w(\vartheta_n, \delta_n) = c_1\vartheta_n^2 + c_2\vartheta_n\delta_n + c_3\delta_n^2 + o((|\vartheta_n| + |\delta_n|)^3),$$

which must satisfy that

$$w(-\vartheta_n + \phi(w(\vartheta_n, \delta_n), \delta_n, \vartheta_n)) = (3-\nu)w(\vartheta_n, \delta_n) + \phi(w(\vartheta_n, \delta_n), \delta_n, \vartheta_n),$$

Thus we can obtain that

$$c_1 = \frac{\sqrt{\nu-2}}{\nu-4},\ c_2 = -\frac{\nu\sqrt{\nu}}{(\nu-2)(\nu-4)} \text{ and } c_3 = 0$$

and the map is restricted to the center manifold, which is given by

$$\begin{aligned} f_3 \ : \ \vartheta_{n+1} = &-\vartheta_n - \frac{4\sqrt{\nu}\sqrt{\nu-2}}{\nu-4}\vartheta_n\delta_n + \frac{3}{2}\frac{(\nu-2)}{(\nu-4)}\vartheta_n^2 + \frac{\nu(2\nu-4+(\nu+2)\sqrt{\nu})}{(\nu-4)^2\sqrt{\nu-2}}\vartheta_n^2\delta_n \\ &-\frac{2\nu^3}{(\nu-2)(\nu-4)^2}\vartheta_n\delta_n^2 - \frac{(\nu^2-4)}{(\nu-4)^2}\vartheta_n^3 + o((|\vartheta_n|+|\delta_n|)^4) \end{aligned}$$

Since

$$\begin{aligned} \alpha_1 &= (\frac{\partial f_3}{\partial \delta_n}\frac{\partial^2 f_3}{\partial \vartheta_n^2} + 2\frac{\partial^2 f_3}{\partial \vartheta_n \partial \delta_n}) \big|_{(0,0)} = -\frac{8\sqrt{\nu}\sqrt{\nu-2}}{\nu-4} \neq 0 \text{ for } \nu \neq 2,\ 4 \\ \alpha_2 &= (\frac{1}{2}(\frac{\partial^2 f_3}{\partial \vartheta_n^2})^2 + \frac{1}{3}\frac{\partial^3 f_3}{\partial \vartheta_n^3}) \big|_{(0,0)} = \frac{\nu^2-36\nu+68}{4(\nu-4)^2} \neq 0 \text{ for } \nu \neq 2, 4 \end{aligned}$$

It is clear that $\alpha_2 > 0$ when $\nu < 2$ and $\alpha_2 < 0$ when $\nu > 2$. Then fixed point E_1 is a subcritical flip bifurcation point of map (1) when $\nu < 2$, whereas the map (1) undergoes a supercritical bifurcation if $\nu > 2$. This completes the proof.

Next, the Neimark-Sacker bifurcation at E_1 will be discussed.

2.2.1 Neimark-Sacker bifurcation

Consider the following two-dimensional map:

$$X_{n+1} = F(X_n, \alpha) \tag{7}$$

where $X_n = (x_n, y_n)$ and $F_\alpha = (f(x_n, y_n, \alpha), g(x_n, y_n, \alpha))$ be a one-parameter family of map of R^2. The map (7) exhibits Neimark-Sacker bifurcation (discrete Hopf bifurcation) if a simple pair of complex conjugate eigenvalues of the linearized map crosses the unit circle [4,10].

In order to study the Neimark-Sacker bifurcation of the interior fixed point of studied map, the following Theorem must be consider firstly.

Theorem 6 *(Neimark-Sacker bifurcation [11-13]). Let F_α be a one parameter family of map of R^2 satisfying :*

(i) $F_\alpha(0) = 0$ for α near 0;

(ii) $DF_\alpha(0)$ has two complex eigenvalues $\lambda(\alpha)$, $\overline{\lambda}(\alpha)$ for α near 0 with $|\lambda(0)| = 1$;

(iii)$\frac{d|\lambda(\alpha)|}{d\alpha}\big|_{\alpha=0} > 0$;

(iv) $\lambda = \lambda(0)$ is not an m-th root of unity for $m = 1, 2, 3, 4$.

Then there is a smooth $\alpha-$dependent change of coordinates bring F_α into the form

$$F_\alpha(X) = G_\alpha(U) + O(|U|^5) \qquad \text{for} \qquad U \in R^2$$

where $U = (u, v)$ and $G = (g_1, g_{2)}$.

Moreover, for all sufficiently small positive (negative) α, F_α has an attracting (repelling) invariant circle if $l(0) < 0$ $(l(0) > 0)$ respectively; and $l(0)$ is given by the following formula:

$$l(0) = -Re[\frac{(1-2\lambda)\overline{\lambda}^2}{(1-\lambda)}\gamma_{20}\gamma_{11}] - \frac{1}{2}|\gamma_{11}|^2 - |\gamma_{02}|^2 + Re(\overline{\lambda}\gamma_{21}). \tag{8}$$

where

$$\begin{aligned}
\gamma_{20} &= \frac{1}{8}[(g_{1uu} - g_{1vv} + 2g_{2uv}) + i(g_{2uu} - g_{2vv} - 2g_{1uv})],\\
\gamma_{11} &= \frac{1}{4}[(g_{1uu} + g_{1vv}) + i(g_{2uu} + g_{2vv})],\\
\gamma_{02} &= \frac{1}{8}[(g_{1uu} - g_{1vv} - 2g_{2uv}) + i(g_{2uu} - g_{2vv} + 2g_{1uv})],\\
\gamma_{21} &= \frac{1}{16}[(g_{1uuu} + g_{1uvv} + g_{2uuv} + g_{2vvv}) + i(g_{2uuu} + g_{2uvv} - g_{1uuv} - g_{1vvv})].
\end{aligned}$$

The calculation of $l(0)$ is given by Wan [12].

2.2.2 Neimark-Sacker bifurcation of fixed point $E_1(-\mu, \sqrt{\mu\nu})$

In this subsection we discuss the Neimark-Sacker bifurcation for fixed point $E_1(-\mu, \sqrt{\mu\nu})$ by using above theorem. The Jacobian matrix of the map (1) at the fixed point E_1 is

$$J(E_1) = \begin{pmatrix} 1-\nu & -2\sqrt{\mu\nu} \\ \sqrt{\mu\nu} & 1 \end{pmatrix}. \tag{9}$$

The characteristic equation of the map (1) at the point E_1 is

$$\lambda^2 - (2-\nu)\lambda + (1 - \nu + 2\mu\nu) = 0. \tag{10}$$

The eigenvalues of $J(E_1)$ are

$$\lambda_{1,2} = \frac{1}{2}(2 - \nu \pm i\sqrt{8\mu\nu - \nu^2}) \text{ for } \mu > \frac{\nu}{8}, \tag{11}$$

and

$$|\lambda_{1,2}| = \sqrt{1 - \nu + 2\mu\nu}. \tag{12}$$

Let $\mu_0 = \frac{1}{2}$, thus

$$\frac{d(|\lambda_{1,2}|)}{d\mu}\,|_{\mu=\mu_0} = \nu.$$

Thus, Neimark-Sacker bifurcation exists when $\nu > 0$, and $|\lambda_{1,2}(\mu_0)| = 1$ and $\lambda_{1,2}(\mu_0) = \frac{1}{2}(2 - \nu \pm i\sqrt{4\nu - \nu^2})$. If $\lambda_{1,2}^m \neq 1$ for $m = 1, 2, 3, 4$. By the following transformation: $\zeta_n = x_n + \mu,\ \eta_n = y_n - \sqrt{\mu\nu}$ under which the map (1) becomes

$$\begin{cases} \zeta_{n+1} = (1-\nu)\zeta_n - 2\sqrt{\nu\mu}\,\eta_n - \eta_n^2, \\ \eta_{n+1} = \sqrt{\mu\nu}\zeta_n + \eta_n + \zeta_n\eta_n. \end{cases} \tag{13}$$

Let

$$\begin{pmatrix} \zeta_n \\ \eta_n \end{pmatrix} = T \begin{pmatrix} u_n \\ \vartheta_n \end{pmatrix},$$

where

$$T = \begin{pmatrix} 1 & 0 \\ -\dfrac{\sqrt{\nu}}{4\sqrt{\mu}} & \dfrac{\sqrt{8\mu\nu - \nu^2}}{4\sqrt{\mu\nu}} \end{pmatrix},$$

under which the map (13) becomes

$$\begin{pmatrix} u_{n+1} \\ \vartheta_{n+1} \end{pmatrix} = \begin{pmatrix} 1 - \dfrac{\nu}{2} & -\dfrac{\sqrt{8\mu\nu - \nu^2}}{2} \\ \dfrac{\sqrt{8\mu\nu - \nu^2}}{2} & 1 - \dfrac{\nu}{2} \end{pmatrix} \begin{pmatrix} u_n \\ \vartheta_n \end{pmatrix} + \begin{pmatrix} g_1(u_n, \vartheta_n) \\ g_2(u_n, \vartheta_n) \end{pmatrix} \tag{14}$$

where

$$\begin{aligned} g_1(u_n,\vartheta_n) &= -\frac{\nu}{16\mu}u_n^2+\frac{\sqrt{8\mu\nu-\nu^2}}{8\mu}u_n\vartheta_n-\frac{8\mu\nu-\nu^2}{16\mu\nu}\vartheta_n^2 \\ g_2(u_n,\vartheta_n) &= -\frac{16\mu\nu+\nu^2}{16\sqrt{8\mu\nu-\nu^2}}u_n^2+(1+\frac{\nu}{8\mu})u_n\vartheta_n\frac{\sqrt{8\mu\nu-\nu^2}}{8}\vartheta_n^2. \end{aligned}$$

Note that (10) is exactly in the form on the center manifold, in which the coefficient l [9]. By using (10) we have

$$\begin{aligned} \gamma_{20}\Big|_{\mu_0=\frac{1}{2}} &= \frac{3}{8\sqrt{4\nu-\nu^2}}(\sqrt{4\nu-\nu^2}-\nu i); \\ \gamma_{11}\Big|_{\mu_0=\frac{1}{2}} &= -\frac{1}{4\sqrt{4\nu-\nu^2}}(\sqrt{4\nu-\nu^2}+3i); \\ \gamma_{02}\Big|_{\mu_0=\frac{1}{2}} &= -\frac{1}{8\sqrt{4\nu-\nu^2}}((\nu+1)\sqrt{4\nu-\nu^2}+(\nu^2-\nu)i); \\ \gamma_{21}\Big|_{\mu_0=\frac{1}{2}} &= 0. \end{aligned}$$

and substituting into (8), we can obtain

$$l=-\frac{(3\nu^3-6\nu^2-24\nu-27)}{32(\nu^2-4\nu)}<0,\ \nu\neq 4$$

From the above analysis, we have the following proposition:

Proposition 7 *the map (1) undergoes a Neimark-Sacker bifurcation at the fixed point* $E_1(-\mu,\sqrt{\mu\nu})$ *if* $\nu^2-8\mu\nu<0$, $\nu>0$ *and* $\mu_0=\frac{1}{2}$, $\nu\neq 4$. *Moreover, an attracting invariant closed curve bifurcates from the fixed point for* $\mu>\frac{1}{2}$.

We will not discuss the bifurcations of point E_2 , because it has symmetrical structure with E_1 , and has similar situation..

3 Controlling Neimark-Sacker bifurcations by using polynomial functions

Various methods have been used to control bifurcations in discrete dynamical systems. Bifurcation control has been designed for fixed points [14], discrete Hopf [15], period doubling bifurcations [16]. All of these method are reviewed by Chen and Yu in [4]. Chen and Yu are designed a nonlinear feedback control with polynomial functions to control a discrete Hopf bifurcations (Neimark-Sacker) in discrete time systems and applied this method in some systems delay logistic map, two dimensional Henon map and three dimensional Henon map [4].

In this section we applied the same technique [4] to control our map about Neimark-Sacker bifurcation. As deduced by proposition that a stable Neimark-Sacker bifurcation occurs at $\mu=0.5$. It is clear that, a stable closed orbit in the phase space(see Figure 1).

Based on the above work, we may choose control component for first equation of the map (1). We can explicitly write the controller as

$$k_n=A_{11}x_n(x_n+\mu)^2+A_{12}y_n(y_n^2-\mu^2),$$

which preserves the three fixed points of the map (1). Then the controlled system given by

$$\begin{cases} x_{n+1}=-y_n^2+A_{11}x_n(x_n+\mu)^2+A_{12}y_n(y_n^2-\mu^2), \\ y_{n+1}=(1+\mu)y_n+x_ny_n. \end{cases} \tag{15}$$

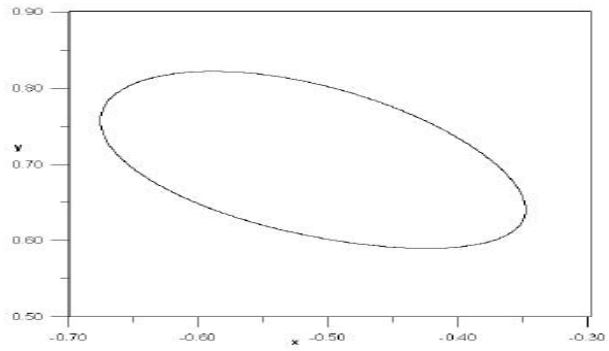

Figure 1: The first stable closed orbit in the map (1) without control for $\mu = 0.51$.

The Jacobian matrix of the map (15) evaluated at $E_1(-\mu, \sqrt{\mu})$ is

$$\begin{pmatrix} 0 & -2\sqrt{\mu} + 2\mu A_{12} \\ \sqrt{\mu} & 1 \end{pmatrix}. \tag{16}$$

The controlled system has a Neimark-Sacker bifurcation when the eigenvalues of (16) satisfied $\lambda_1 = \overline{\lambda}_2$ and $|\lambda_1| = 1$. The necessary condition for (16) to have a pair complex eigenvalues is

$$A_{12} < \frac{8\mu - 1}{8\mu\sqrt{\mu}}$$

Thus we may further choose $A_{12} = \frac{1}{2}$, $A_{11} = 0$ and $\mu = 1$. Then the Jacobian matrix evaluated at E_1 of controlled system becomes

$$\begin{pmatrix} 0 & -1 \\ 1 & 1 \end{pmatrix}$$

This matrix indicates that the Neimark-Sacker bifurcation occurs at $\mu = 1$ for the controlled map (15) instead of the Neimark-Sacker bifurcation occurs at $\mu = \frac{1}{2}$ for uncontrolled map (1). By using above choice the map (15) becomes

$$\begin{cases} x_{n+1} = -y_n^2 + \frac{1}{2}y_n^3 - \frac{1}{2}y_n, \\ y_{n+1} = 2y_n + x_n y_n. \end{cases} \tag{17}$$

Let $\zeta_n = x_n + 1$ and $\eta_n = y_n - 1$, then the controlled map (17) becomes

$$\begin{cases} \zeta_{n+1} = -\eta_n + \frac{1}{2}\eta_n^2 + \frac{1}{2}\eta_n^3, \\ \eta_{n+1} = \zeta_n + \eta_n + \zeta_n\eta_n. \end{cases} \tag{18}$$

We can deduced that

$$T = \begin{pmatrix} 1 & 0 \\ -\frac{1}{2} & \frac{\sqrt{3}}{2} \end{pmatrix}.$$

By the following transformation

$$\begin{pmatrix} \zeta_n \\ \eta_n \end{pmatrix} = T \begin{pmatrix} u_n \\ \vartheta_n \end{pmatrix}$$

the map (18) becomes

$$\begin{pmatrix} u_{n+1} \\ \vartheta_{n+1} \end{pmatrix} = \begin{pmatrix} \frac{1}{2} & -\frac{\sqrt{3}}{2} \\ \frac{\sqrt{3}}{2} & \frac{1}{2} \end{pmatrix} \begin{pmatrix} u_n \\ \vartheta_n \end{pmatrix} + \begin{pmatrix} \frac{1}{8}u_n^2 - \frac{\sqrt{3}}{4}u_n\vartheta_n + \frac{3}{8}\vartheta_n^2 - \frac{1}{16}u_n^3 + \frac{3\sqrt{3}}{16}u_n^2\vartheta_n - \frac{9}{16}u_n\vartheta_n^2 + \frac{3\sqrt{3}}{16}\vartheta_n^3, \\ -\frac{7}{8\sqrt{3}}u_n^2 + \frac{3}{4}u_n\vartheta_n + \frac{\sqrt{3}}{8}\vartheta_n^2 - \frac{1}{16\sqrt{3}}u_n^3 + \frac{3}{16}u_n^2\vartheta_n - \frac{3\sqrt{3}}{16}u_n\vartheta_n^2 + \frac{3}{16}\vartheta_n^3. \end{pmatrix}$$

Note that (15) is exactly in the form on the center manifold. By simple computation and using Eq. (4), we have

$$\gamma_{20} = \frac{1}{8\sqrt{3}}(\sqrt{3} - i); \gamma_{11} = \frac{1}{4\sqrt{3}}(\sqrt{3} - i); \gamma_{02} = -\frac{1}{4\sqrt{3}}(\sqrt{3} + 2i); \gamma_{21} = -\frac{\sqrt{3}}{8}i.$$

Thus, $l = -\frac{1}{32} < 0$.

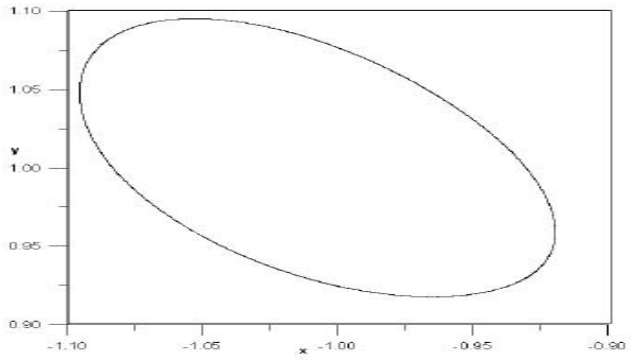

Figure 2: The first stable closed orbit in the controlled map (18) for $\mu = 1.1$.

Since $l < 0$, the Neimark-Sacker bifurcation of the controlled map is a stable. The numerical simulation result is shown in Figure 2, confirming the existence of a stable closed orbit in the phase space. From above analysis, we deduce that the feedback controller polynomial function delays the appearance of Neimark-Sacker bifurcation and control the map around stable closed orbit.

4 Numerical Simulations

In this section, some numerical simulation results are presented to confirm the previous analytic results and to obtain even more dynamics behaviors of the map (1). To do this, we will use the bifurcation diagrams, phase portraits, Lyapunov exponents and Sensitive dependence on initial conditions and show the new interesting complex dynamical behaviors. The bifurcation parameters are considered in the following three cases :

(i) varying μ in range $0 \leq \mu < 1$, and fixing $\nu = 1$.

(ii) varying μ in range $0 \leq \mu < 1,$ and fixing $\nu = 2$.

(iii) varying μ in range $0 \leq \mu < 1,$ and fixing $\nu = 0.5$.

For case (i). Let $\nu = 1$, the bifurcation diagram of x with respect to μ is presented in Figure 3. This Figure shows that the pitchfork bifurcation occurs at $\mu = 0$, i.e., with the increase of the parameter μ, the stable fixed point $E_0(0, 0)$ loses its stability at $\mu = 0$. When $\nu = 1$, $\mu = \frac{1}{2}$, according to the theoretical analysis given in section 2.2 , a Neimark-Sacker bifurcation should occur. This result has been proved by the numerical simulation is shown in Figure 3.

We give the bifurcation diagram of the map (1) with $\nu = 1$ in $(\mu - y)$ plane covering range $\mu \in [0, 0.99]$ in Figure 4 and the local amplification for $\mu \in [0.68, 0.72]$ in Figure 5 . Infact, the fixed points E_1 and E_2 of the map (1) losetheir stability at Neimark-Sacker bifurcation value at $\mu = \frac{1}{2}$, so there is appearing of an invariant circles when $\mu \geq \frac{1}{2}$.

Figures 3-5 show the dynamical behaviors of the map (1) become complex when the parameter $\mu > \frac{1}{2}$. Lyapunov exponents measure the exponential rates of convergence or divergence, in time, of adjacent trajectories in phase space. In order to analyze the parameter sets for which stable, periodic and chaotic behavior, one can compute the maximal Lyapunov exponents depend on μ . For the stable fixed points the maximal Lyapunov exponents is negative. For quasiperiodic, invariant closed curve the maximal Lyapunov exponents is zero. For chaotic behavior the maximal Lyapunov exponents is positive. The maximal Lyapunov exponents corresponding to Figures 3-4 computed and presented in Figure 6.

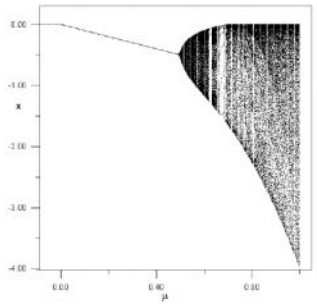

Figure 3: Bifurcation diagram in $(\mu - x)$ plane for $\nu = 1$.

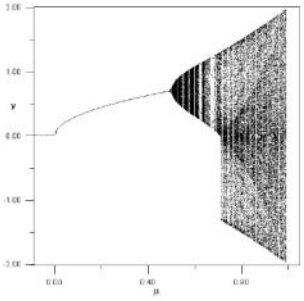

Figure 4: Bifurcation diagram in $(\mu - y)$ plane for $\nu = 1$.

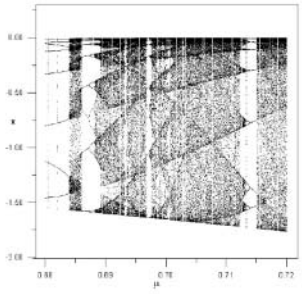

Figure 5: Local amplification corresponding to 3.

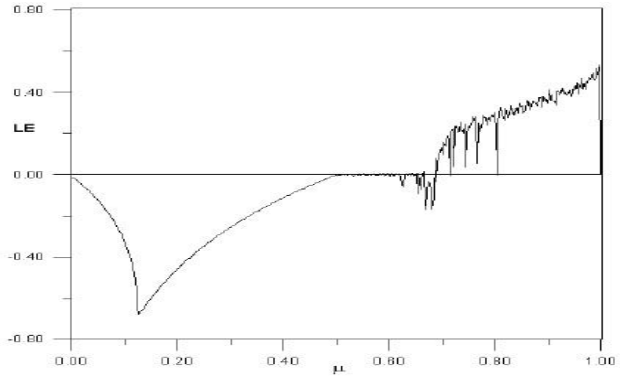

Figure 6: Maximal Lyapunov exponents corresponding to Fig.3 and 4.

From Figure 6, one can see that the maximal Lyapunov exponents is in neighborhood of zero for $\mu \in [0, .65]$, which corresponds to fixed points or continuous closed invariant circles. When $\mu \in (0.65, 1)$ the maximal Lyapunov exponents is positive which corresponding to chaotic behavior.
For case (ii). The bifurcation diagram of map (6.1) in ($\mu - y$) plane for $\nu = 2$ is shown in Figure 6.7. The bifurcation diagram of the map (1) in ($\mu - x$) plane for $\nu = 2$ is disposed in Figure 8. From this figure its clear that the flip bifurcation emerges from the fixed point $(-0.5, 1)$.

The maximal Lyapunov exponents corresponding to Figures 7, 8 is given in Figure 9, showing the period orbits and the existence of chaotic regions as the parameter μ varying.

Case (iii), The bifurcation diagram of the map (1) in ($\mu - x$) plane for $\nu = 0.5$ is plotted in Figure 10, Also maximal Lyapunov exponents is disposed in Figure 10. The Neimark-Sacker bifurcation emerges from the fixed points $(-0.5, 0.5)$ at $\nu = 0.5$. It shows the correctness of Proposition 7.

From proposition 7, we deduced that the first Neimark-Sacker bifurcation takes place for $\mu = \frac{1}{2}$ and for

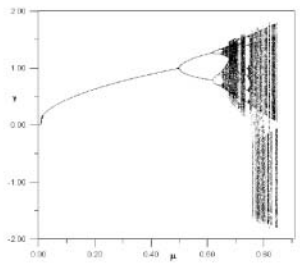

Figure 7: Bifurcation diagram in $(\mu - y)$ plane for $\nu = 2$.

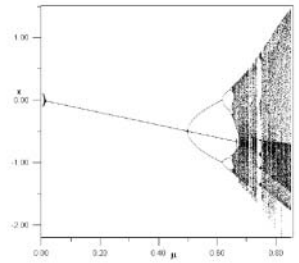

Figure 8: Bifurcation diagram in $(\mu - x)$ plane for $\nu = 2$.

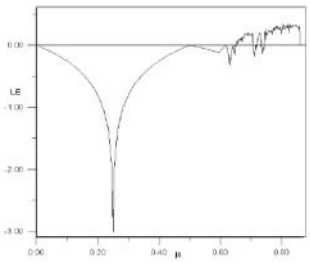

Figure 9: Maximal Lyapunov exponents corresponding to Fig.7 and 8.

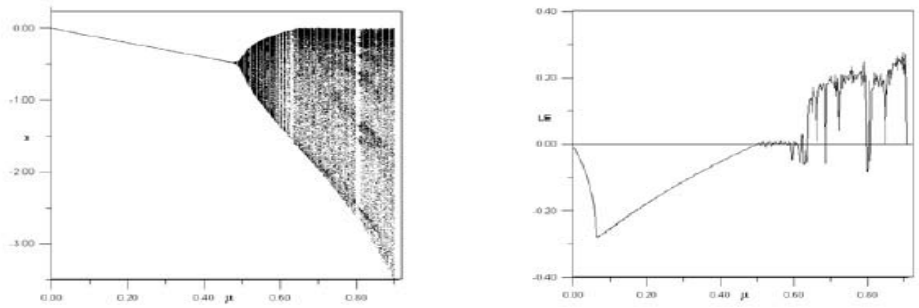

Figure 10: Bifurcation diagram in $(\mu - x)$ plane for $\nu = 0.5$ and corresponding Maximal Lyapunov exponents .

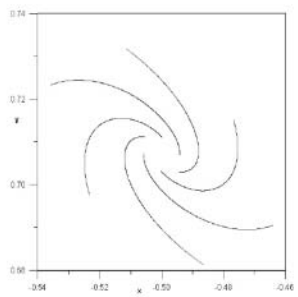

Figure 11: The first Neimark-Sacker bifurcation when $\mu = 0.5$.

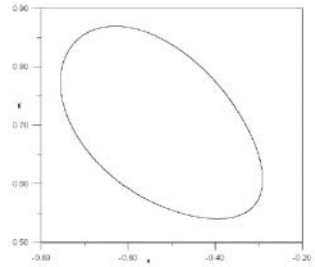

Figure 12: The invariant closed curve around the fixed point E_1 created after Neimark-Sacker bifurcation when $\mu = 0.52$.

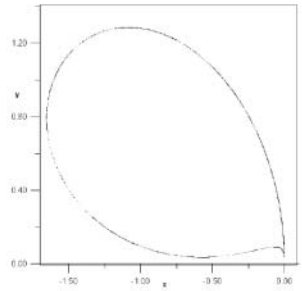

Figure 13: The breakdown of the invariant closed curve when $\mu = 0.7$.

values lower than $\mu = \frac{1}{2}$ a stable fixed points exists. For $\mu = \frac{1}{2}$ and $\nu = 1$ the fixed point E_1 occurs at $x = -\frac{1}{2}$, $y = 0.707$ and the associated pair of complex conjugate eigenvalues are $\lambda_{1,2} = \frac{1}{2} \pm \frac{\sqrt{3}}{2}i$ with $|\lambda_{1,2}| = 1$, which shows that the first Neimark-Sacker bifurcation occurs at $\mu = \frac{1}{2}$ as shown in Figure. 11.

Continuing to increase the value of μ , we see what happens for $\mu = 0.52$ and $\nu = 1$. One can see that the fixed point E_1 became unstable and an invariant closed curve was created around the fixed point E_1, as shown in the Figure 12.

The breakdown of the invariant closed curve around the fixed point E_1 when $\mu = 0.7$ and $\nu = 1$ shown in Figure 13.

Further increases in μ the chaotic attractors arises. A typical double chaotic attractors presented in Figure 14, with $\mu = 0.83$ and $\nu = 1$, one chaotic attractor around fixed point E_1 and the other one is around E_2 .

In addition, Figure 15 shows more complex double chaotic attractorswith $\mu = 0.88$ and $\nu = 1$.

When $\mu = 0.9999$ and $\nu = 1$, invariant disc will appear due to a contact bifurcation between the attractor and its basin boundary see Figure 16. The invariant disc disappear when $\mu = 1$. From Figure 16 its clear that the existence of an invariant circle and invariant absolutely continuous measure on the disc bounded by this circle. It is true that the measure of the whole disc is infinitely large because the corresponding density is nonintegrable, the integral of this density logratithmicaly diverges near the boundary. In computer simulation, one can observe the longtime walking of iterations on the disc, but later all of them leave the disc and go to infinity. This caused by transverse instability of the invariant boundary circle. It follows particularly from the existence of unstable fixed points $(0, 0)$, $(-1, \pm 1)$ (and others unstable cycles) on its boundary. After iterates arrive in a sufficiently small vicinity of such unstable fixed point or cycle they leave the disc with a good probability because of round-of errors, see V. Tsybulin and V. Yudovich [17].

At $\nu = 1.5$, the phase portraits corresponding to $\mu = 0.45,\ 0.5, 0.6, 0.75$, and 0.85 are shown in Figure 17(1)-(5) respectively. We see that the fixed points of the map (1) are stable for $\mu < 0.5$, and loses stability at $\mu = 0.5$, an invariant closed curve appears when the parameter μ exceeds 0.5 . There is an invariant

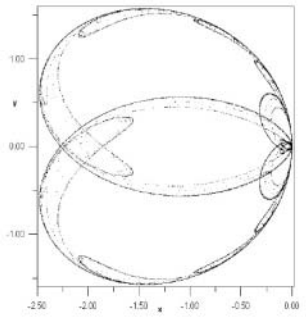

Figure 14: Double chaotic attractor when $\mu = 0.83$.

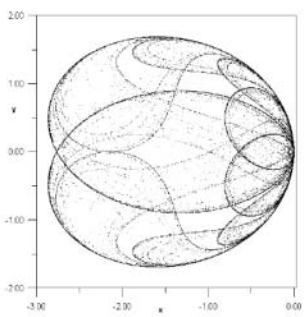

Figure 15: Double chaotic attractor when $\mu = 0.88$.

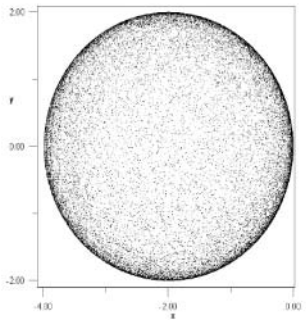

Figure 16: Invariant disc(full developed chaos) when $\mu = 0.999$.

closed curve for more large regions of $\mu \in (0.5, 0.72)$. When μ increases there are orbits of higher order and attracting chaotic sets.

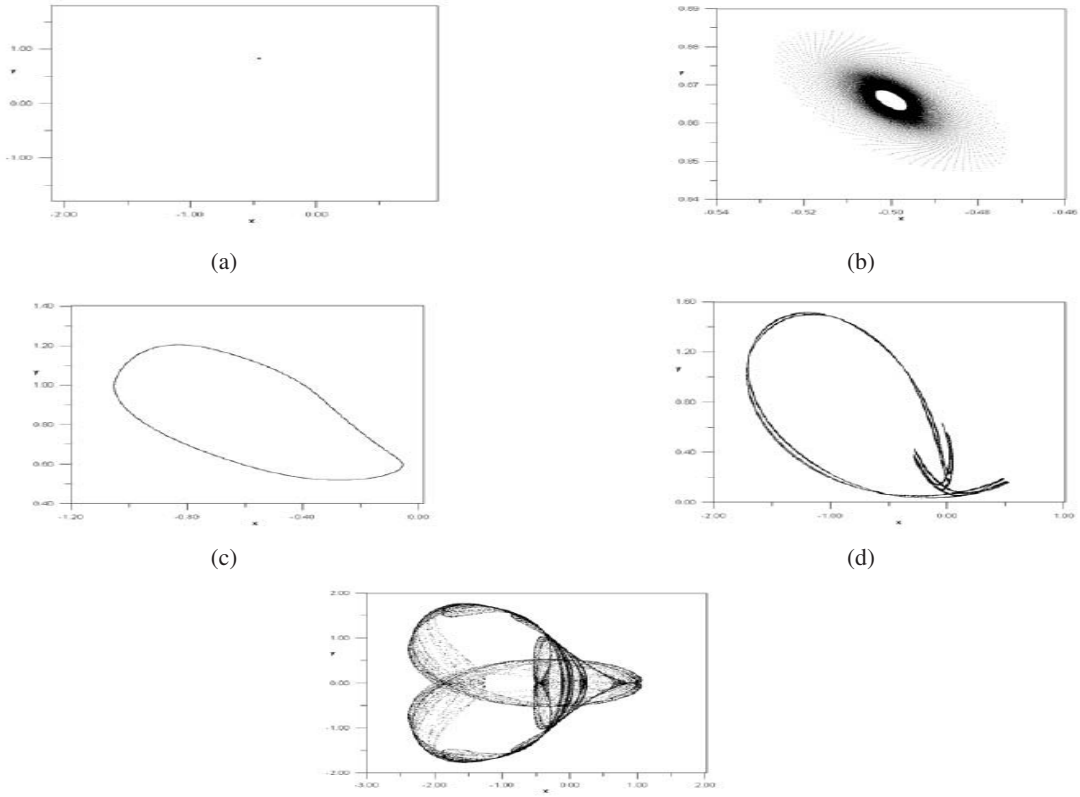

(a) (b) (c) (d) (e)

Figure 17: Phase portraits for various values of μ when $\nu = 1.5$.

In Figure 18, we see three typical chaotic attractors of the map (1) associated with the three cases (i)-(iii).

From above analysis one can deduce that Burgers mapping contains very rich nonlinear dynamics when its parameters are varied. Many forms of complexities are observed such as chaotic bands (including periodic windows, pitchfork bifurcation, flip bifurcation, Neimark-Sacker bifurcation and attractors crisis) and chaotic attractors.

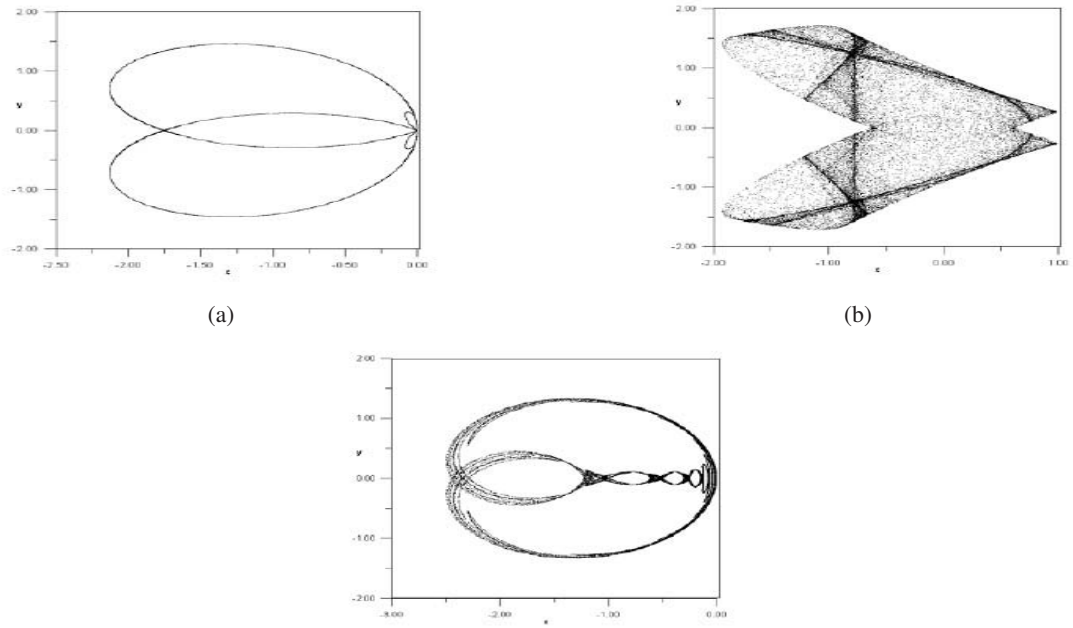

(a) (b)

(c)

Figure 18: Phase portraits for various values of ν when $\mu = 0.78$.

4.1 Sensitive dependence on initial conditions

To demonstrate the sensitivity to the initial conditions of the Burgers mapping, two orbits with initial points (x_0, y_0) and $(x_0+0.0001, y_0)$ are computed, respectively,and are represented in Figure 19. At the beginning, the two time series are overlapped and are undistinguishable; but after a number of iterations, the difference between them builds up rapidly. Fig. 19 shows a sensitive dependence on initial conditions for $x-$ coordinate of the two orbits for the model (1), which is plotted against the time with the parameter value $\mu = 0.73$ and $\nu = 2$. The difference between the two $x-$ coordinates is 0.0001 , while the other coordinate is kept to has the same value. For this case the two orbits with initial points $(-0.04, 0.2)$ and $(-0.0401, 0.2)$ are computed respectively and plotted in Figure 19 as a function of time.

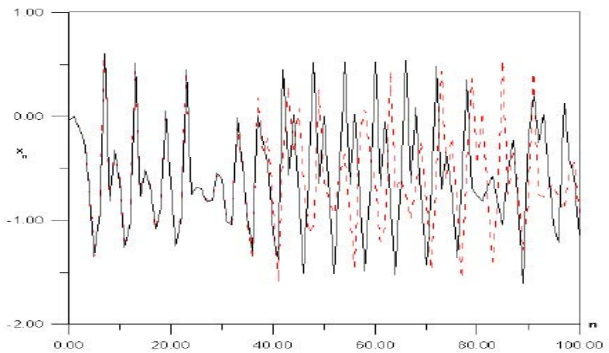

Figure 19: Sensitive dependence on initial conditions for map (1),x-coordinates of the two orbits,plotted against time;the x-coordinates of initial condition differ by 0.0001,and the other coordinate kept equal.

Also, the sensitive dependence on initial conditions, $y-$ coordinates of the two orbits, for the map (1), are plotted against the time in Figure 20. The $y-$ coordinate of initial conditions differs by 0.0001 ,while the

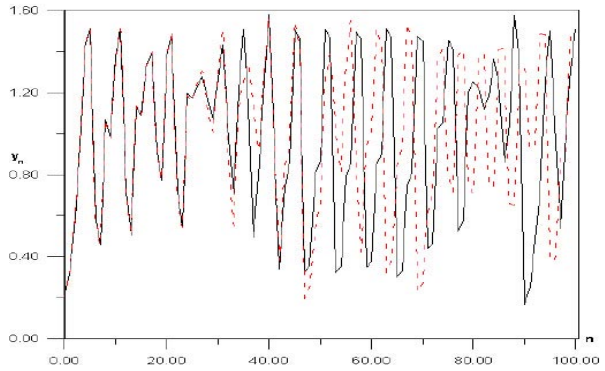

Figure 20: Sensitive dependence on initial conditions for map(1),y-coordinates of the two orbits,plotted against time;the y-coordinates of initial condition differ by 0.0001,and the other coordinate kept equal.

other coordinate is kept at the same value. From Figures 19 and 20 it is shown that the time series of the map (1) is a sensitive dependence to initial conditions, i.e. complex dynamic behaviors occur in this map.

5 Conclusions

In this paper, we have analyzed the dynamical behaviors for Burgers mapping map in $\mathbb{R}^2$, and found many complex and interesting dynamical behaviors. Our theoretical analysis have demonstrated that the map (1) undergoes pitchfork bifurcation, flip bifurcation and Neimark-Sacker bifurcation. We controlled the map around stable Neimark-Sacker bifurcation by using feedback polynomial controller method. Numerical simulations carried out to verify our theoretical analysis.

Acknowledgments

One of us (A. Elsadany) thanks Z. J. Jing, Y. Zhang and H. Cao for sending their some works papers.

References

[1] J. M. Burgers: Mathematical examples illustrating relations occurring in the theory of turbulent fluid motion.*Trans. Roy. Neth. Acad. Sci. Amsterdam.* 17:1-53(1939)

[2] R. R. Whitehead, N. MacDonald: Introducing students to nonlinearity: computer experiments with Burgers mappings. *Eur. J. Phys.* 6:143-147(1985)

[3] R. R. Whitehead, N. MacDonald: A chaotic map that displays its own homoclinic structure.*Physica D.* 13:401-408(1984)

[4] Z. Chen, P. Yu: Controlling and anti-controlling Hopf bifurcations in discrete maps using polynomial functions.*Chaos, Solitons & Fractals.* 26:1231-1248(2005)

[5] Z. J. Jing, Z. Jia, R. Wang: Chaos bihavior in the discrete BVP oscillator. *Int J Bifurcat& Chaos.* 12:619-627(2002)

[6] Z. J. Jing, Y. Chang, B. Guo: Bifurcation and chaos discrete FitzHugh-Nagumo system. *Chaos & Solitons & Fractals.* 21: 701-720(2004)

[7] Z. J. Jing, J. Yang: Bifurcation and chaos discrete-time predator-prey system. *Chaos & Solitons & Fractals.* 27: 259-277(2006)

[8] H. Sun, H. Cao: Bifurcations and chaos of a delayed ecological model.*Chaos, Solitons & Fractals.* 4:1383-1393(2007)

[9] Y. Zhang, Q. Zhang, L. Zhao, C. Yang: Dynamical behaviors and chaos control in a discrete functional response model. *Chaos, Solitons & Fractals.*4:1318-1327(2007)

[10] G. Iooss: Bifurcation of maps and applications. *North-Holland, Amsterdam.* (1977)

[11] Y. Chang, X. Li: Dynamical behaviors in a two-dimensional map. *Acta Math App Sinica Engl Ser.* 19: 663-676(2003)

[12] Y.H. Wan: Computation of the stability condition for the Hopf bifurcation of diffeomorphism on R^2. *SIAM. J. Appl. Math.* 34:167-175(1978)

[13] J. Guckenheimer, P. Holmes: Nonlinear oscillations, dynamical systems, and bifurcations of vectors.*New York: Springer-Verlag.*(1983)

[14] K.C. Yap, GR. Chen, T. Ueta: Controlling bifurcations of discrete maps. *latin Amer Appl Res.* 31:157-162(2001)

[15] E.H. Abed, J.H. Fu: Local feedback stabilization and bifurcation control. *I. Hopf bifurcation. Syst Contr Lett* 7:11-17(1986)

[16] E.H. Abed, H.O. Wang, GR. Chen: Stabilization of period doubling bifurcations and implications for control of chaos. *Physica D.* 70:150-164(1994)

[17] V. Tsybulin, V. Yudovich: Invariant setes and attractors of quadratic mapping of plane computer experiment and anlytical treatment.*Int. J. Difference Equations and Applications.* 4: 397-324(1998)